Received: 11 January 2019 | Revised: 24 April 2019 | Accepted: 30 April 2019

DOI: 10.1002/aoc.5007

FULL PAPER

WILEY Applied Organometallic Chemistry

Derivatization of valproic acid using ferrocene derivatives: Synthesis, characterization and investigation of optical and electrochemical properties

Keshvar Rahimpour[1,2] | Abolghasem Jouyban[1] | Reza Teimuri-Mofrad[2]

[1] Pharmaceutical Analysis Research Center and Faculty of Pharmacy, Tabriz University of Medical Sciences, Tabriz, Iran

[2] Department of Organic and Biochemistry, Faculty of Chemistry, University of Tabriz, Tabriz, Iran

Correspondence
Keshvar Rahimpour, Department of Organic and Biochemistry, Faculty of Chemistry, University of Tabriz, Tabriz, Iran.
Email: k.rahimpour@tabrizu.ac.ir

New ferrocenyl-based valproic acid (VPA) ester derivatives were designed and synthesized according to the reaction of appropriate haloalkylferrocene derivatives with VPA in the presence of K_2CO_3 and a catalytic amount of 18-crown-6 ether. Elemental analyses and Fourier transform infrared, ^{1}H NMR, ^{13}C NMR and mass spectra all well confirmed the predicted molecular structure. This is the first report in which ferrocene has been applied in derivatization of VPA as a chromogenic group. The electrochemical properties of the synthesized compounds were studied using cyclic voltammetry measurements, and energies of the frontier molecular orbitals were determined. In addition, the solubilities of the final compounds were studied in distilled water, phosphate buffer (pH = 7.4) and 0.9% (w/v) NaCl solution.

KEYWORDS
cyclic voltammetry, ferrocene, valproic acid, visible spectrophotometry

1 | INTRODUCTION

Valproic acid (VPA; 2-propylpentanoic acid) is a synthetic analogue of valeric acid, a short-chain fatty acid which in the form of its sodium salt is widely used in the treatment of neurologic disorders. The most well-known use is as an antiepileptic drug and mood stabilizer.[1] Also, it has been demonstrated that VPA can act as a histone deacetylases inhibitor.[2] Furthermore, VPA shows anti-inflammatory and antioxidative properties.[3]

The therapeutic concentration range of VPA in plasma is considered to be about 50–100 μg ml^{-1}. There are various methods for monitoring VPA concentrations in biological fluids (plasma, urine, etc.) and the monitoring of VPA concentration is required to ensure the effectiveness of drugs and to avoid adverse reactions.[4] Known methods of VPA determination in clinical applications include immunoassay,[5] high-performance liquid chromatography with UV detection[6] and fluorescence detection,[7] MS,[8] capillary electrophoresis[9] and additionally GC because of the volatility of VPA.[10]

Most of these methods are based on prior derivatization to add a suitable chromophore or fluorophore to the VPA structure, since it is a simple saturated eight-carbon branched-chain fatty acid without any chromogenic group. A number of fluorescence- and UV-sensitive reagents including bromoacetophenone derivatives and methoxycoumarin-based compounds have been employed for derivatization of VPA and other short-chain fatty acids (C_6–C_9).[11–13]

Ferrocene derivatives with high optical absorptivity, good thermal and photochemical stability, ease of functionalization and favourable electrochemical properties have found many practical applications in materials science including catalysts,[14] medicines,[15] sensors,[16] aerospace[17] and electroactive materials.[18]

Based on our previous works on linear and nonlinear optical properties of ferrocenyl compounds,[19–23] we

decided to use the potential usefulness of highly UV-sensitive ferrocene derivatives for a simple and convenient derivatization and determination of VPA.

2 | EXPERIMENTAL

2.1 | General methods

Commercial compounds were used without further purification. Column chromatography was performed using SiO_2 (60 Å, 230–400 mesh, particle size 0.040–0.063 mm) at 25°C. ^{1}H NMR and ^{13}C NMR spectra were obtained with Bruker FT-400 and 100 MHz spectrometers, respectively (Supporting Information). The chemical shifts were referenced to the residual solvent as follows: $CHCl_3$ = 7.26 ppm (^{1}H), 76.0 ppm (^{13}C). For ^{1}H NMR, the resonance multiplicity was described as s (singlet), d (doublet), t (triplet) and m (multiplet). Fourier transform infrared (FT-IR) spectra were recorded with band intensities indicated as s (strong), m (medium) and w (weak) with a Bruker-Tensor 270 spectrometer. Mass spectra were obtained with an Agilent 5975C VL instrument operated at 70 eV, the most important peaks being reported in m/z units with M^+ as the molecular ion. Iron analysis was performed with an Analytik Jena Novaa 400 atomic absorption spectrophotometer and UV–visible spectra were recorded with an Analytik Jena SPECORD 250 UV–visible spectrophotometer. Elemental analyses were carried out with an Elementor Vario ELIII instrument. Cyclic voltammetry (CV) measurements were performed using 1 mM solutions of ferrocene derivatives in acetonitrile in the presence of 0.100 M $LiClO_4$, as supporting electrolyte, using a a potentiostat/galvanostat (Autolab PGASTAT 30) equipped with a standard three-electrode cell. A glassy carbon electrode of 2 mm in diameter was used as the working electrode. A silver/silver chloride (Ag/AgCl) electrode and a platinum electrode were used as the reference and the counter electrodes, respectively. All potentials in this study were measured with respect to Ag/AgCl.

2.2 | Synthesis of chloroalkylferrocenes and bromoalkylferrocenes

2-Chloroacetylferrocene (**2a**), 3-chloropropionylferrocene (**2b**), 4-chlorobutyroylferrocene (**2c**), 2-chloroethylferrocene (**3a**), 3-chloropropylferrocene (**3b**), 4-chlorobutylferrocene (**3c**), 2-bromoethylferrocene (**4a**), 3-bromopropylferrocene (**4b**) and 4-bromobutylferrocene (**4c**) were prepared according to procedures described previously.[24,25]

2.3 | General procedure for synthesis of iodide derivatives of ferrocene

A solution of 1 mmol of sodium iodide in 15 ml of dry acetone was added to a solution of 1 mmol of the appropriate chloroalkyl-substituted ferrocenyl compound in 20 ml of the same solvent. This clear mixture was stirred at room temperature until a precipitate of sodium chloride was formed. The reaction mixture was filtered and, after evaporation of acetone, crude product was obtained in >95% yield. The obtained compounds had acceptable purity for subsequent steps.

2.3.1 | 2-Iodoethylferrocene (5a)

Using 0.1 g (0.40 mmol) of **3a**, 0.13 g (0.39 mmol) of dark orange liquid (97% yield) was obtained. ^{1}H NMR (400 MHz, $CDCl_3$, 25°C, δ, ppm): 4.16 (s-br, 9H), 3.28–3.25 (t, 2H), 2.80–2.78 (t, 2H). ^{13}C NMR (100 MHz, $CDCl_3$, 25 °C, δ, ppm): 83.52, 68.23, 67.58, 67.44, 36.52, 5.2. FT-IR (KBr, cm^{-1}): 3082 (w), 2935–2861 (s), 649 (m), 496 (w). Anal. Calcd for $C_{12}H_{13}FeI$ (%): C, 42.39; H, 3.85; Fe, 16.42. Found (%): C, 42.41; H, 3.86; Fe, 16.43.

2.3.2 | 3-Iodopropylferrocene (5b)

Using 0.1 g (0.38 mmol) of **3b**, 0.13 g (0.37 mmol) of dark orange liquid (98% yield) was obtained.[26] ^{1}H NMR (400 MHz, $CDCl_3$, 25°C, δ, ppm): 4.13–4.08 (d, 9H), 3.21–3.19 (t, 2H), 2.55–2.49 (t, 2H), 1.09–1.02 (m, 2H). ^{13}C NMR (100 MHz, $CDCl_3$, 25°C, δ, ppm): 83.45, 68.83, 68.23, 67.49, 33.19, 31.62, 28.43, 6.73. FT-IR (KBr, cm^{-1}): 3082 (w), 2925–2855 (s), 648 (m), 494 (w). Anal. Calcd for $C_{13}H_{15}FeI$ (%): C, 44.11; H, 4.26; Fe, 15.77. Found (%): C, 44.11; H, 4.25; Fe, 15.75.

2.3.3 | 4-Iodobutylferrocene (5c)

Using 0.1 g (0.36 mmol) of **3c**, 0.12 g (0.34 mmol) of dark orange liquid (96% yield) was obtained.[26] ^{1}H NMR (400 MHz, $CDCl_3$, 25°C, δ, ppm): 4.14–4.09 (d, 9H), 3.24–3.20 (t, 2H), 2.40–2.36 (t, 2H), 1.86–1.79 (m, 2H), 1.72–1.64 (m, 2H). ^{13}C NMR (100 MHz, $CDCl_3$, 25°C, δ, ppm): 86.75, 67.58, 67.15, 66.52, 30.32, 27.95, 7.24. FT-IR (KBr, cm^{-1}): 3082 (w), 2933–2862 (m), 649 (m), 496 (w). Anal. Calcd for $C_{14}H_{17}FeI$ (%): C, 45.68; H, 4.65; Fe, 15.17. Found (%): C, 45.67; H, 4.66; Fe, 15.18.

2.3.4 | 2-Iodoacetylferrocene (5d)

Using 0.1 g (0.38 mmol) of **2a**, 0.12 g (0.36 mmol) of dark orange solid (96% yield) was obtained. M.p. 78–79°C. ^{1}H NMR (400 MHz, $CDCl_3$, 25 C, δ, ppm): 4.84–4.83 (t, 2H), 4.59–4.58 (t, 2H), 4.25 (s, 5H), 4.13 (s, 2H). ^{13}C NMR (100 MHz, $CDCl_3$, 25°C, δ, ppm): 195.97, 79.27, 72.05, 69.25, 69.16, 2.07. FT-IR (KBr, cm^{-1}): 3106 (w), 2926–2855 (m), 1642 (s), 670 (m), 522 (w). Anal. Calcd for $C_{12}H_{11}FeIO$ (%): C, 40.72; H, 3.13; Fe, 15.77. Found (%): C, 40.74; H, 3.12; Fe, 15.78.

2.4 | General procedure for synthesis of ferrocenyl-based VPA ester derivatives

Sodium valproate salt was dissolved in deionized water, acidified with H_2SO_4 and extracted with hexane. After evaporation of hexane, 1 mmol of liquid VPA was added to a solution of 1 mmol of appropriate haloalkyl-substituted ferrocenyl compound in 10 ml of acetonitrile. Amounts of 1 mmol of K_2CO_3 and 1 ml of 2×10^{-3} M solution of 18-crown-6 ether in acetonitrile were added and the reaction mixture was refluxed. After completion of the reaction (monitoring with TLC), the solvent was evaporated under reduced pressure, the residue was dissolved in dichloromethane and washed with water. The organic phase was dried over Na_2SO_4, filtered and the solvent was removed under reduced pressure. The crude products were purified by column chromatography on silica gel with hexane–EtOAc as eluent. Specific details for each compound are given in Table 1.

2.4.1 | 2-Ferrocenylethyl 2-propylpentanoate (VPAC2Fc, 6a)

Dark orange liquid. ^{1}H NMR (400 MHz, $CDCl_3$, 25°C, δ, ppm): 4.20–4.11 (m, 11H), 2.63–2.59 (t, 2H), 2.39–2.32 (m, 1H), 1.64–1.54 (m, 2H), 1.47–1.37 (m, 2H), 1.37–1.24 (m, 4H), 0.91–0.88(t, 6H). ^{13}C NMR (100 MHz, $CDCl_3$, 25°C, δ, ppm): 175.44, 84.37, 68.46, 68.16, 67.25, 63.40, 44.26, 33.57, 27.92, 19.59, 12.97. FT-IR (KBr, cm^{-1}): 3094 (w), 2948–2868 (m), 1731 (s), 486 (w). Anal. Calcd for $C_{20}H_{28}FeO_2$ (%): C, 67.42; H, 7.92; Fe, 15.67. Found (%): C, 67.45; H, 7.91; Fe, 15.68. MS (70 eV): $m/z = 356$ $[M]^+$.

TABLE 1 Optimal reaction time and obtained yield for ferrocene-based VPA ester derivatives

	Optimal time (h)			Yield (%)		
Compound	**Cl**	**Br**	**I**	**Cl**	**Br**	**I**
VPAC2Fc (**6a**)	24	5	2	80	95	100
VPAC3Fc (**6b**)	24	5	2	80	95	100
VPAC4Fc (**6c**)	24	5	2	80	95	100
VPACOFc (**6d**)	12	2	<1	100	100	100

2.4.2 | 3-Ferrocenylpropyl 2-propylpentanoate (VPAC3Fc, 6b)

Dark orange liquid. ^{1}H NMR (400 MHz, $CDCl_3$, 25°C, δ, ppm): 4.11–4.05 (m, 11H), 2.41–2.35 (m, 3H), 1.88–1.80 (m, 2H), 1.64–1.57 (m, 2H), 1.46–1.25 (m, 6H), 0.93–0.90 (t, 6H). ^{13}C NMR (100 MHz, $CDCl_3$, 25°C, δ, ppm): 175.56, 87.01, 67.68, 67.07, 66.23, 62.51, 44.32, 33.68, 29.08, 24.89, 19.64, 13.01. FT-IR (KBr, cm^{-1}): 3096 (w), 2930–2858 (m), 1734 (s), 513 (w). Anal. Calcd for $C_{21}H_{30}FeO_2$ (%): C, 68.11; H, 8.16; Fe, 15.08. Found (%): C, 68.09; H, 8.15; Fe, 15.08. MS (70 eV): $m/z = 370$ $[M]^+$.

2.4.3 | 4-Ferrocenylbutyl 2-propylpentanoate (VPAC4Fc, 6c)

Brown liquid. ^{1}H NMR (400 MHz, $CDCl_3$, 25°C, δ, ppm): 4.10–4.06 (m, 11H), 2.38–2.32 (m, 3H), 1.69–1.52 (m, 6H), 1.45–1.24 (m, 6H), 0.91–0.88 (t, 6H). ^{13}C NMR (100 MHz, $CDCl_3$, 25°C, δ, ppm): 175.62, 88.76, 68.31, 67.74, 66.83, 62.88, 44.35, 33.69, 28.17, 27.58, 26.38, 19.65, 13.00. FT-IR (KBr, cm^{-1}): 3093 (w), 2941–2866 (m), 1731 (s), 489 (w). Anal. Calcd for $C_{22}H_{32}FeO_2$ (%): C, 68.75; H, 8.39; Fe, 14.53. Found (%): C, 68.74; H, 8.40; Fe, 14.54. MS (70 eV): $m/z = 384$ $[M]^+$.

2.4.4 | 2-Oxo-2-ferrocenylethyl 2-propylpentanoate (VPACOFc, 6d)

Orange solid. M.p. 79–81°C. ^{1}H NMR (400 MHz, $CDCl_3$, 25°C, δ, ppm): 5.06 (s, 2H), 4.80–4.79 (t, 2H), 4.55–4.54 (t, 2H), 4.29 (s, 5H), 2.58–2.51 (m. 1H), 1.76–1.34 (m, 8H), 0.95–0.92 (t, 6H). ^{13}C NMR (100 MHz, $CDCl_3$, 25°C, δ, ppm): 195.38, 175.00, 81.08, 71.46, 69.23, 67.62, 64.72, 44.07, 33.62, 19.58, 13.07. FT-IR (KBr, cm^{-1}): 3005 (w), 2941–2868 (m), 1735 (s), 1670 (s), 470 (w). Anal. Calcd for $C_{20}H_{26}FeO_3$ (%): C, 64.88; H, 7.07; Fe, 15.08. Found (%): C, 64.86; H, 7.06; Fe, 15.09. MS (70 eV): $m/z = 370$ $[M]^+$.

2.5 | Solubility determination

The solid–liquid equilibrium in distilled water, phosphate buffer solution (150 mM, pH 7.4) and 0.9% (w/v) solution of NaCl was investigated using the shake-flask

technique.[27] An excess amount of each of the synthesized compounds **6a**–**d** was introduced into a glass vessel filled with about 5 g of the solvent under investigation and then the vial was located in an incubator (Kimia Idea Pardaz Azarbayjan (KIPA) Co., Iran) at definite temperatures and allowed to equilibrate for 48 h on a shaker (Behdad, Iran). At the end of the equilibration time, the saturated solutions were centrifuged (Eppendorf centrifuge model 5810R, Germany), diluted with 96% ethanol (if necessary) and analysed at 266 nm for **6d** and 203 nm for **6a**–**c** using a UV–visible spectrophotometer (UV-1800, Shimadzu, Japan). The absorbance of the diluted solutions was recorded and the concentrations were calculated using a previously constructed UV spectrophotometric calibration curve. Each experimental data point was a mean of three experimental measurements.

2.6 | Computational methods

Molar solubility values of the synthesized compounds in the investigated solvents at various temperatures were fitted by the van't Hoff equation with the help of equation (1):[28]

$$\ln C_T = A + \frac{B}{T} \tag{1}$$

Here, C_T is the molar solubility of solute in the selected solvent at given temperature T and the terms A and B are the model constants.

For comparison and the investigation of the quality of the back-calculated data by the investigated numerical analysis, the mean relative deviation (MRD) was calculated using equation (2):

$$\text{MRD}\ (\%) = \frac{100}{N}\sum\left(\frac{\left|C_{\text{m}}^{\text{Cal}} - C_{\text{m}}^{\text{Obs}}\right|}{C_{\text{m}}^{\text{Obs}}}\right) \tag{2}$$

where N denotes the number of experimental data points in each dataset.

2.7 | Thermodynamic analysis of dissolution

The dissolution behaviours of the synthesized compounds in the desired solvents were investigated by computing of the apparent thermodynamic parameters (i.e. dissolution standard enthalpy (ΔH°), entropy (ΔS°) and Gibbs free energy change (ΔG°)) on the basis of the van't Hoff and Gibbs equations. The modified version of the van't Hoff equation is

$$\frac{\partial \ln C}{\partial\left(\frac{1}{T}-\frac{1}{T_{\text{m}}}\right)_p} = -\frac{\Delta H^\circ}{R} \tag{3}$$

where C is the molar solubility of solute and T and R are the absolute temperature (K) and ideal gas constant, respectively.[29] T_{hm} is the mean harmonic temperature computed using equation (4):

$$T_{\text{hm}} = \frac{n}{\sum_{i=1}^{n}(1/T)} \tag{4}$$

where n is the number of investigated temperatures. In this case, the obtained T_{hm} value is 303.0 K. By plotting ln C versus $1/T - 1/T_{\text{hm}}$, the values of ΔH° and ΔG° of dissolution can be computed from the slope and the intercept, respectively,[29] and ΔS° as a function of the degree of disorder of a system can be obtained using the Gibbs equation.

The relative contributions of enthalpy (ζ_H) and entropy (ζ_{TS}) to ΔG° of the dissolution process are calculated using equations (5) and (6):[30]

$$\zeta_H = \frac{|\Delta H^\circ|}{(|\Delta H^\circ| + |T\Delta S^\circ|)} \tag{5}$$

$$\zeta_{TS} = \frac{|T\Delta S^\circ|}{(|\Delta H^\circ| + |T\Delta S^\circ|)} \tag{6}$$

3 | RESULTS AND DISCUSSION

3.1 | Chemistry

Sensitive determination of VPA in biological fluids is usually achieved with pre-column derivatization due to the lack of a chromogenic group in the VPA structure. To the best of our knowledge, ferrocene derivatives have never been used in this area. Well-defined electrochemical properties and the ability to absorb a wide range of visible light wavelengths prompted us to incorporate ferrocenyl units with VPA and investigate the optical and electrochemical properties of resulting compounds.

At first, commercially available sodium valproate salt was dissolved in deionized water and acidified using H_2SO_4; at approximately pH 5.0 the solution becomes cloudy meaning the formation of VPA. Based on the literature, *n*-hexane is a suitable organic solvent for extraction of VPA.[31] Thus we extracted VPA and removed the *n*-hexane using a rotary evaporator at reduced pressure. With the precursor VPA in hand, we focused on the

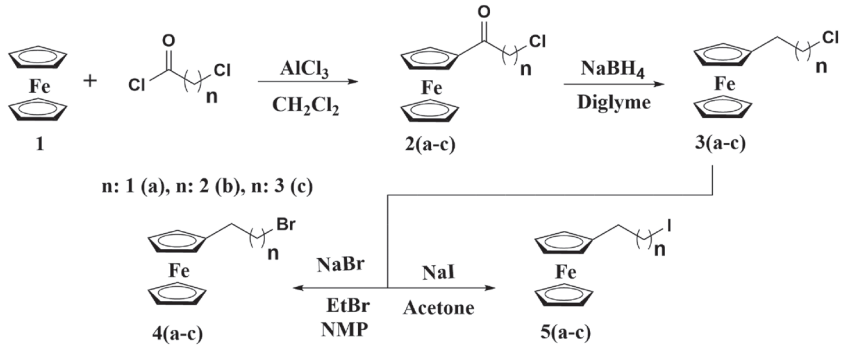

SCHEME 1 Synthesis of haloalkyl-substituted ferrocenyl derivatives

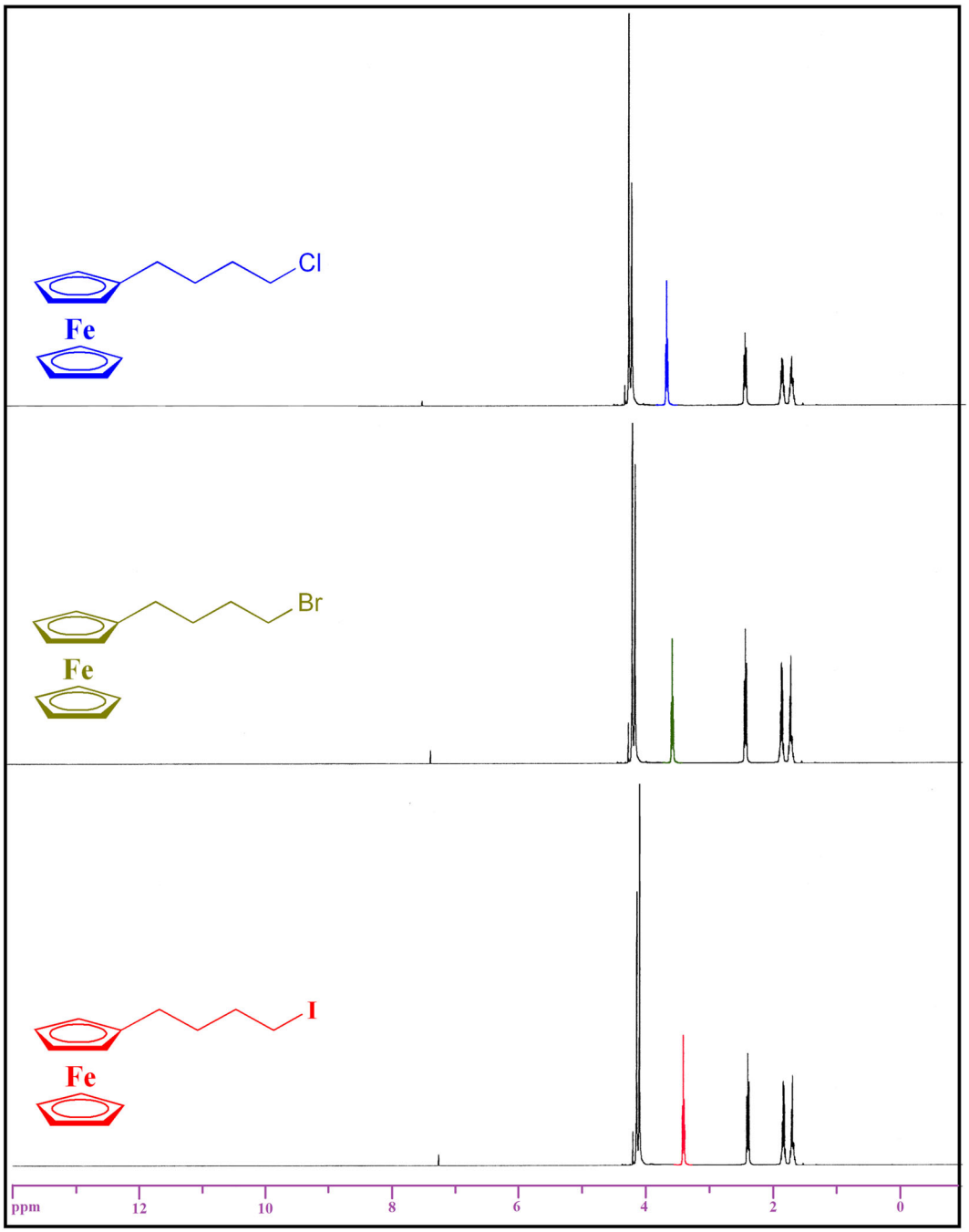

FIGURE 1 ^{1}H NMR spectra for 4-halobutylferrocene derivatives

feasibility of the reaction between haloalkyl-substituted ferrocenyl derivatives and VPA.

Scheme 1 exhibits the synthetic route for the preparation of haloalkyl-substituted ferrocenyl derivatives.

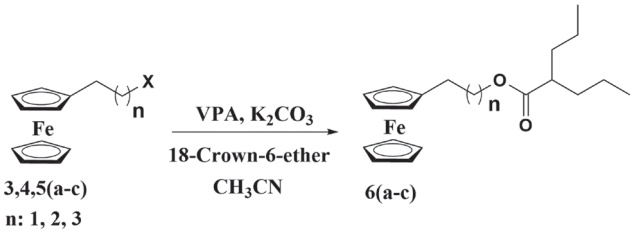

SCHEME 2 Synthesis of valproate ester derivatives

Friedel–Crafts acylation of ferrocene along with reduction of related acyls to alkyls lead to the synthesis of chloroalkyl-substituted ferrocene derivatives. Bromination was carried out in *N*-methyl-2-pyrrolidone (NMP) as solvent using NaBr and ethyl bromide, and iodination was performed in acetone with sodium iodide. ^{1}H NMR spectroscopy was used to follow the halogen exchange reactions from chemical shift information. Figure 1 depicts the ^{1}H NMR spectra for 4-halobutylferrocene derivatives. As might be expected, the obvious upfield shift for methylene protons in the vicinity of halides on passing from Cl to Br and I is in agreement with electronegativity values, $\Delta\delta$ = 3.54 ppm for 4-chlorobutylferrocene,

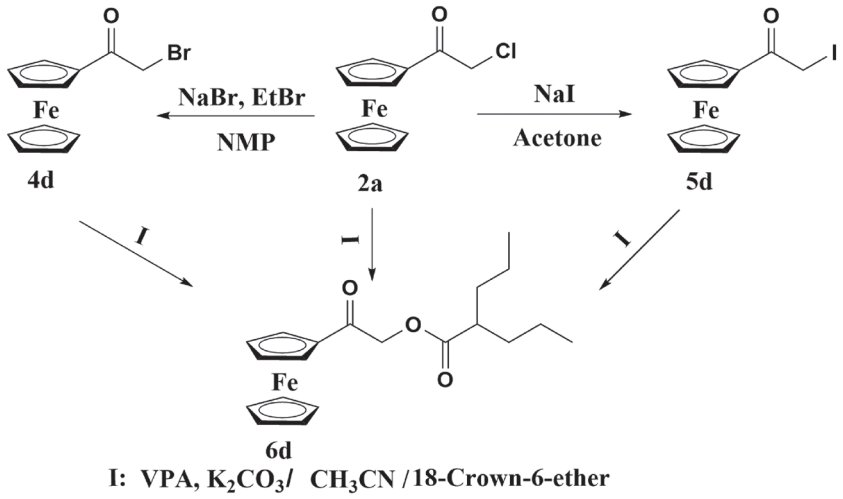

SCHEME 3 Synthesis of 2-oxo-2-ferrocenylethyl 2-propylpentanoate (VPACOFc)

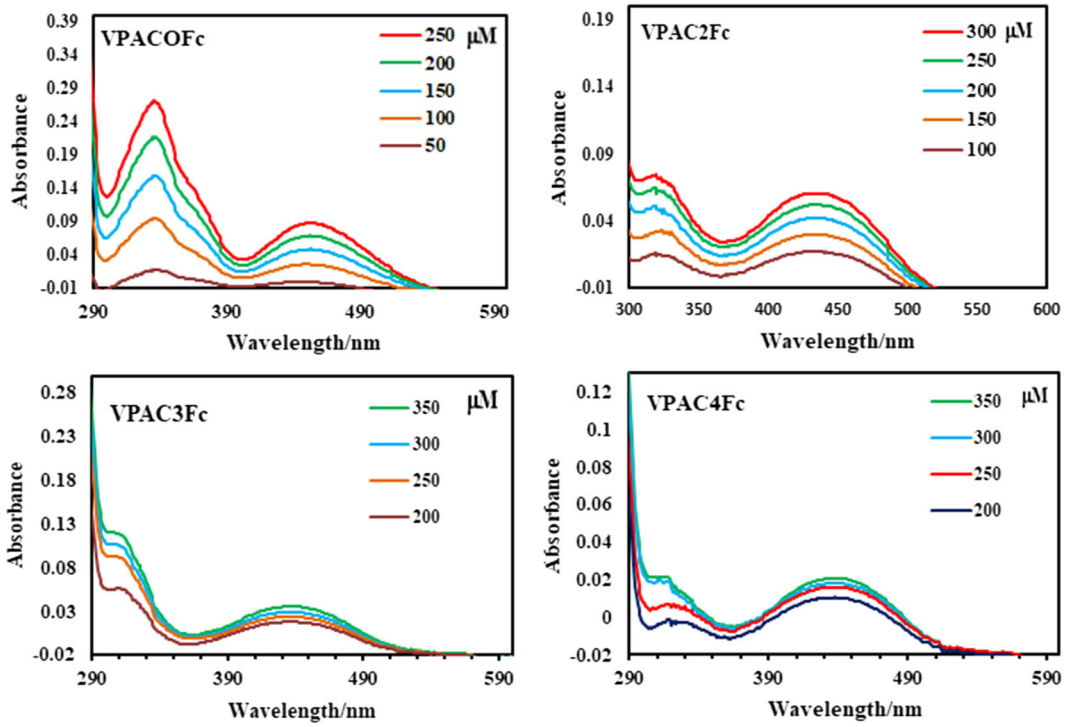

FIGURE 2 UV–visible spectra of ferrocenyl-based VPA ester derivatives in acetonitrile solution

$\Delta\delta$ = 3.44 ppm for 4-bromobutylferrocene and $\Delta\delta$ = 3.22 ppm for 4-iodobutylferrocene, as assigned in Figure 1. These series are expected for all of the synthesized haloalkylferrocene derivatives.

Schemes 2 and 3 illustrate the reaction of haloalkylferrocene derivatives with VPA in acetonitrile, a water-miscible solvent, in the presence of K_2CO_3. The VPA molecule was converted to potassium valproate in alkaline solution. In general a nucleophilic reaction is found to be significantly faster in the presence of 18-crown-6 ether, and therefore we used this catalytic system for the preparation of ferrocene-based VPA derivatives. Table 1 presents the required time and obtained yield for each compound when we used different halides derivatives as starting material. It is evident that with an increase of leaving group ability, the reaction time was decreased and the yield was improved. Under similar conditions the length of alkyl chain did not have any significant effect on reaction time and yield, but 2-haloacetylferrocene shows the best result for each case. It seems that the presence of carbonyl group in the vicinity of leaving halide facilitates the halogen replacement.

The absorption spectra of the ferrocene derivatives in the range 300–600 nm are shown in Figure 2. All the spectra display two absorption bands resulting from π–π^* and metal-to-ligand charge transfer transitions of the ferrocene moiety. Absorption intensity of VPACOFc (**6d**) is higher than that of the alkylic derivatives to the extent that a 50 μM solution of it can be detected. In the case of **6a** this concentration is limited to 100 μM and for propyl and butyl ester derivatives (**6b** and **6c**) is limited to 200 μM and lower concentrations are not detectable.

The electrochemical properties of the synthesized derivatives were investigated using CV with a solution of 0.1 M lithium perchlorate in anhydrous acetonitrile.

TABLE 2 CV data for 1.0 mM solutions of ferrocenyl-based VPA ester derivatives

Compound	E_{pc}	E_{pa}	ΔE_p	i_{pc}/i_{pa}
VPAC2Fc (**6a**)	0.33	0.42	0.08	0.82
VPAC3Fc (**6b**)	0.31	0.39	0.07	0.84
VPAC4Fc (**6c**)	0.30	0.38	0.08	0.50
VPACOFc (**6d**)	0.63	0.718	0.08	0.61

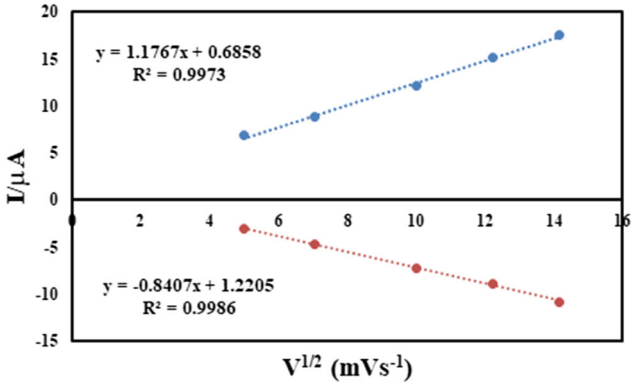

FIGURE 4 Linear relationship between cathodic–anodic peak current and square root of scan rate for VPACOFc as representative of the synthesized compounds

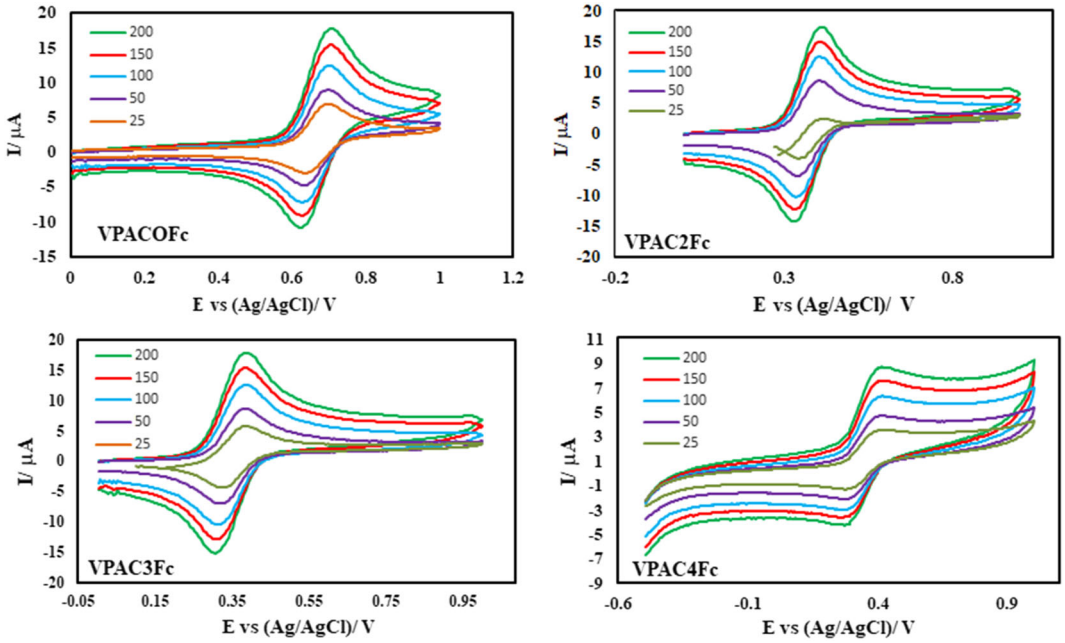

FIGURE 3 CV curves of ferrocenyl-based VPA ester derivatives at various scan rates (scan rates given in mV s^{-1})

Figure 3 shows the CV curves for the synthesized VPA ester derivatives. These compounds are electrochemically active, and in each case, the CV curves show one pair of symmetric redox peaks corresponding to well-defined Fe(II)/Fe(III) couple with peak-to-peak separation values ($\Delta E_p = E_{pa} - E_{pc}$) ≤ 0.08 V at scan rates up to 0.20 V s^{-1} (Table 2). E_p values were independent of the scan rate and anodic–cathodic peak current ratios were in the range $0.50 < i_{pc}/i_{pa} < 0.84$. In all cases, a plot of peak current versus $v^{1/2}$ (where v is the scan rate) was linear, indicating that redox processes were diffusion controlled (Figure 4).

In addition, the highest occupied molecular orbital (HOMO) energy levels for the synthesized compounds were calculated according to equation (7):

$$E_{HOMO} = -[E_{ox} + 4.8 - E_{ferrocene}] \quad (7)$$

TABLE 3 Energies of frontier molecular orbitals (HOMO and LUMO)

Entry	HOMO	LUMO	E_g
VPAC2Fc (**6a**)	−4.81	−2.48	2.33
VPAC3Fc (**6b**)	−4.77	−2.45	2.32
VPAC4Fc (**6c**)	−4.75	−2.44	2.31
VPACOFc (**6d**)	−5.09	−2.74	2.34

where E_{ox} is the onset potential of oxidation in CV curves and $E_{ferrocene}$ is the onset potential of ferrocene oxidation versus Ag/AgCl ($E_{ferrocene}$ = 0.27 in acetonitrile). Lowest

TABLE 5 The van't Hoff equation constants and MRD for the back-calculated solubility of synthesized compounds in investigated solvents

Synthesized compound	*A*	*B*	MRD (%)
Water			
VPACOFc (**6d**)	22.231	−9540.006	22.5
VPAC2Fc (**6a**)	4.250	−5263.226	13.0
VPAC3Fc (**6b**)	−1.558	−3281.596	1.44
VPAC4Fc (**6c**)	27.149	−12273.677	20.0
Phosphate buffer (pH 7.4)			
VPACOFc (**6d**)	17.264	−7662.221	17.5
VPAC2Fc (**6a**)	−4.098	−2632.685	5.2
VPAC3Fc (**6b**)	−3.196	−2605.148	2.1
VPAC4Fc (**6c**)	10.178	−6964.983	6.4
0.9% NaCl solution			
VPACOFc (**6d**)	16.458	−7275.118	10.9
VPAC2Fc (**6a**)	10.515	−7268.556	7.4
VPAC3Fc (**6b**)	−3.979	−2523.853	2.1
VPAC4Fc (**6c**)	39.756	−16585.581	16.6

TABLE 4 Experimental values of molar solubility of synthesized compounds in investigated solvents at various temperatures

Synthesized compound	*T* (K)	Solubility (mol L^{-1})		
		Water	Phosphate buffer (pH 7.4)	0.9% NaCl solution
VPACOFc (**6d**)	293.2	6.52×10^{-5}	1.08×10^{-4}	1.96×10^{-4}
	298.2	2.14×10^{-4}	2.77×10^{-4}	4.72×10^{-4}
	303.2	3.20×10^{-4}	4.05×10^{-4}	5.25×10^{-4}
	308.2	4.66×10^{-4}	4.87×10^{-4}	7.38×10^{-4}
	313.2	5.84×10^{-4}	6.48×10^{-4}	1.13×10^{-3}
VPAC2Fc (**6a**)	293.2	1.30×10^{-6}	1.94×10^{-6}	6.80×10^{-7}
	298.2	1.42×10^{-6}	2.61×10^{-6}	9.03×10^{-7}
	303.2	1.74×10^{-6}	2.93×10^{-6}	1.27×10^{-6}
	308.2	2.41×10^{-6}	3.30×10^{-6}	2.36×10^{-6}
	313.2	4.22×10^{-6}	3.52×10^{-6}	3.05×10^{-6}
VPAC3Fc (**6b**)	293.2	2.89×10^{-6}	5.73×10^{-6}	4.01×10^{-6}
	298.2	3.45×10^{-6}	6.46×10^{-6}	4.79×10^{-6}
	303.2	4.29×10^{-6}	7.74×10^{-6}	5.71×10^{-6}
	308.2	5.07×10^{-6}	8.43×10^{-6}	6.21×10^{-6}
	313.2	5.82×10^{-6}	1.02×10^{-5}	6.99×10^{-6}
VPAC4Fc (**6c**)	293.2	3.29×10^{-7}	1.17×10^{-6}	3.87×10^{-8}
	298.2	8.77×10^{-7}	2.10×10^{-6}	1.68×10^{-7}
	303.2	2.13×10^{-6}	2.91×10^{-6}	3.61×10^{-7}
	308.2	3.65×10^{-6}	3.72×10^{-6}	8.12×10^{-7}
	313.2	4.49×10^{-6}	5.84×10^{-6}	1.59×10^{-6}

TABLE 6 Thermodynamic quantities of solution processes of synthesized compounds in different solvents at T_{hm}

Synthesized compound	$\Delta G°$ (kJ mol^{-1})	$\Delta H°$ (kJ mol^{-1})	$\Delta S°$ (J mol^{-1} K^{-1})	$T\Delta S°$ (kJ mol^{-1})	ζ_H	ζ_{TS}
Water						
VPACOFc (**6d**)	20.79	79.29	193.07	58.50	0.58	0.42
VPAC2Fc (**6a**)	33.05	43.76	35.35	10.71	0.80	0.20
VPAC3Fc (**6b**)	31.21	27.20	−13.24	−4.01	0.87	0.13
VPAC4Fc (**6c**)	33.65	102.05	225.73	68.40	0.60	0.40
Phosphate buffer (pH 7.4)						
VPACOFc (**6d**)	20.22	63.85	144.00	43.63	0.59	0.41
VPAC2Fc (**6a**)	32.21	21.91	−33.98	−10.30	0.68	0.32
VPAC3Fc (**6b**)	29.71	21.53	−27.00	−8.18	0.72	0.28
VPAC4Fc (**6c**)	32.27	57.98	84.85	25.71	0.69	0.31
0.9% NaCl solution						
VPACOFc (**6d**)	19.02	60.57	137.12	41.55	0.59	0.41
VPAC2Fc (**6a**)	33.94	60.49	87.62	26.55	0.69	0.31
VPAC3Fc (**6b**)	30.54	20.98	−31.54	−9.56	0.69	0.31
VPAC4Fc (**6c**)	37.74	137.87	330.45	100.13	0.58	0.42

unoccupied molecular orbital (LUMO) energy levels were obtained using equation (8):[19]

$$E_{LUMO} = E_{HOMO} + E_g \quad (8)$$

where E_g is the optical band gap which is obtained via electronic absorption spectra. These data are summarized in Table 3.

3.2 | Solubility of synthesized compounds 6a–d and data correlation

As these compounds were prepared with the aim of their use for valproate derivatization in biological fluids, the solubilities of synthesized compounds **6a–d** were studied in distilled water, at physiological pH (phosphate buffer, pH = 7.4) and in isotonic saline solution (0.9% (w/v) NaCl solution), which simulated conditions for biological fluids. The measured molar solubility data of the synthesized compounds in the investigated solutions at various temperatures are listed in Table 4. In all cases, the solubility profile represented a linear increase with increasing temperature. At a given temperature (298.2 K), for the investigated compounds for all used solvents, the solubility decreased in the following order: VPACOFc (**6d**) > VPAC4Fc (**6c**) > VPAC3Fc (**6b**) > VPAC2Fc (**6a**).

The experimental molar solubility results in each solvent were correlated and back-calculated with equation (1). The numerical values of the coefficients of the van't Hoff equation along with the MRD values for the back-calculated solubilities are listed in Table 5. Using this computation, the molar solubility at various temperatures could be calculated with the overall MRD of 17.0% for **6d**, 8.5% for **6a**, 1.9% for **6b** and 14.3% for **6c**.

3.3 | Thermodynamic properties

Table 6 presents the thermodynamic parameters including $\Delta H°$, $\Delta S°$ and $\Delta G°$ of the synthesized compounds dissolved in the various solvents investigated in this work at the harmonic temperature of 303.0 K. The results show that the dissolution process of the compounds in the investigated solvents is endothermic ($\Delta H° > 0$ in all cases), entropy-driven ($\Delta S° > 0$ except for VPAC3Fc in all solvents and VPAC2Fc in phosphate buffer) and apparently not spontaneous ($\Delta G° > 0$ in all cases). The ζ_H and ζ_{TS} values for solvation for the investigated compounds are also presented in Table 6. In all cases, the main contributor to $\Delta G°$ of the dissolution process of the synthesized compounds is $\Delta H°$ ($\zeta_H > \zeta_{TS}$).

4 | CONCLUSIONS

In summary, we report the design and synthesis of some ferrocenyl-based VPA ester derivatives through the reaction of haloalkyl-substituted ferrocenyl derivatives with VPA using a catalytic amount of 18-crown-6 ether. The solubilities of the synthesized compounds **6a–d** were studied in distilled water, phosphate buffer (pH = 7.4) and 0.9% (w/v) NaCl solution. There are no previous reports available on the application of ferrocene as a

labelling reagent in this area. Among the synthesized compounds, VPACOFc (**6d**) shows a good sensitivity in the visible region with a detection limit of 50 μM which is a reasonable concentration for VPA level in clinical applications.

ORCID

Keshvar Rahimpour https://orcid.org/0000-0003-4998-957X
Reza Teimuri-Mofrad https://orcid.org/0000-0002-5812-6445

REFERENCES

[1] L. Shao, L. T. Young, J. F. Wang, *Biol. Psychiatry* **2005**, *58*(11), 879.

[2] J. A. Williams, C. J. Barreiro, L. U. Nwakanma, M. S. Lange, L. E. Kratz, M. E. Blue, J. Berrong, N. D. Patel, V. L. Gott, J. C. Troncoso, M. V. Johnston, *Ann. Thorac. Surg.* **2006**, *81*(6), 2235.

[3] J. C. M. Ximenes, E. C. L. Verde, M. da Graça Naffah-Mazzacoratti, G. S. de Barros Viana, *Neurosci. Med.* **2012**, *3*(01), 107.

[4] K. Matsuura, T. Ohmori, M. Nakamura, Y. Itoh, K. Hirano, *Biomed. Chromatogr.* **2008**, *22*(4), 387.

[5] W. Ehrenthal, M. Rochel, *Arzneimittelforschung* **1982**, *32*(4), 449.

[6] K. Kushida, T. Ishizaki, *J. Chromatogr. B* **1985**, *338*, 131.

[7] M. C. Lin, H. S. Kou, C. C. Chen, S. M. Wu, H. L. Wu, *J. Chromatogr. B* **2004**, *810*(1), 169.

[8] S. Gao, H. Miao, X. Tao, B. Jiang, Y. Xiao, F. Cai, Y. Yun, J. Li, W. Chen, *J. Chromatogr. B* **2011**, *879*(21), 1939.

[9] T. T. T. Pham, H. H. See, R. Morand, S. Krähenbühl, P. C. Hauser, *J. Chromatogr. B* **2012**, *907*, 74.

[10] R. Fazeli-Bakhtiyari, V. Panahi-Azar, M. H. Sorouraddin, A. Jouyban, *Iran J. Basic Med. Sci.* **2015**, *18*(10), 979.

[11] V. Pucci, R. Mandrioli, M. A. Raggi, *Electrophoresis* **2003**, *24*(12–13), 2076.

[12] M. B. Majnooni, B. Mohammadi, R. Jalili, A. Babaei, G. Bahrami, *J. Liq. Chromatogr. Relat. Technol.* **2016**, *39*(19–20), 877.

[13] H. Danafar, M. Hamidi, *Adv. Pharm. Bull.* **2015**, *5*(4), 563.

[14] C. Ornelas, *New J. Chem.* **2011**, *35*(10), 1973.

[15] E. A. Hillard, A. Vessieres, G. Jaouen, *Med. Organometal. Chem.* **2010**, *32*, 81.

[16] M. Saleem, H. Yu, L. Wang, H. Khalid, M. Akram, N. M. Abbasi, J. Huang, *Anal. Chim. Acta* **2015**, *876*, 9.

[17] D. Saravanakumar, N. Sengottuvelan, V. Narayanan, M. Kandaswamy, T. L. Varghese, *J. Appl. Polym. Sci.* **2011**, *119*(5), 2517.

[18] A. K. Diallo, C. Ornelas, L. Salmon, J. Ruiz Aranzaes, D. Astruc, *Angew. Chem. Int. Ed.* **2007**, *46*(45), 8644.

[19] R. Teimuri-Mofrad, K. Rahimpour, R. Ghadari, *J. Organometal. Chem.* **2016**, *811*, 14.

[20] R. Teimuri-Mofrad, K. Rahimpour, R. Ghadari, S. Ahmadi-Kandjani, *J. Mol. Liq.* **2017**, *244*, 322.

[21] R. Teimuri-Mofrad, K. Rahimpour, R. Ghadari, *J. Organometal. Chem.* **2017**, *846*, 397.

[22] R. Teimuri-Mofrad, K. Rahimpour, A. Poursadegh, *Mater. Chem. Phys.* **2017**, *200*, 384.

[23] K. Rahimpour, R. Teimuri-Mofrad, A. Vaez, *Appl. Organometal. Chem.* **2018**, *32*(2), e4031.

[24] a)H. H. Jung, J. R. Carey, E. T. Brower, A. J. Gengenbach, J. A. Abramite, Y. Lu, *J. Am. Chem. Soc.* **2005**, *127*(44), 15356. b)A. P. Ferreira, J. L. F. da Silva, M. T. Duarte, M. F. M. da Piedade, M. P. Robalo, S. G. Harjivan, C. Marzano, V. Gandin, M. M. Marques, *Organometallics* **2009**, *28*(18), 5412.

[25] K. D. Safa, H. Abbasi, R. Teimuri-Mofrad, F. A. Charandabi, *Aust. J. Chem.* **2014**, *67*(5), 784.

[26] V. Jouikov, J. Simonet, *Langmuir* **2011**, *28*(1), 931.

[27] A. Jouyban, M. A. A. Fakhree, in *Toxicity and Drug Testing*, (Ed: W. E. Acree Jr.), Intech Co., New York **2012**.

[28] M. Gantiva, F. Martínez, *Fluid Phase Equilib.* **2010**, *293*, 242.

[29] S. Vahdati, A. Shayanfar, J. Hanaee, F. Martínez, J. Acree, A. Jouyban, *Ind. Eng. Chem. Res.* **2013**, *52*, 16630.

[30] G. L. Perlovich, S. V. Kurkov, A. Eur, *J. Pharm. Sci.* **2003**, *19*, 423.

[31] J. F. Zhang, Z. Q. Zhang, W. C. Dong, Y. Jiang, *J. Chromatogr. Sci.* **2014**, *52*, 1173.

SUPPORTING INFORMATION

Additional supporting information may be found online in the Supporting Information section at the end of the article.

How to cite this article: Rahimpour K, Jouyban A, Teimuri-Mofrad R. Derivatization of valproic acid using ferrocene derivatives: Synthesis, characterization and investigation of optical and electrochemical properties. *Appl Organometal Chem*. 2019;e5007. https://doi.org/10.1002/aoc.5007